SCIENCE CHINA
Earth Sciences

•RESEARCH PAPER•

October 2022 Vol.65 No.10: 2005–2017
https://doi.org/10.1007/s11430-021-9943-y

Accurate analysis of Cu isotopes by fs-LA-MC-ICP-MS with non-matrix-matched calibration

Nan LV[1], Zhian BAO[1], Kaiyun CHEN[1], Kai WU[1] & Honglin YUAN[1,2*]

[1] *State Key Laboratory of Continental Dynamics, Department of Geology, Northwest University, Xi'an 710069, China;*
[2] *Collaborative Innovation Center of Continental Tectonics, Xi'an 710069, China*

Received November 26, 2021; revised March 8, 2022; accepted April 20, 2022; published online August 26, 2022

Abstract The copper isotopic compositions of 12 copper-rich minerals (including native copper, sulfides, carbonates, oxides, and copper chloride) have been determined using a 206 nm ultraviolet femtosecond laser ablation multi-collector inductively coupled plasma mass spectrometry (UV-fs-LA-MC-ICP-MS). A pure copper wire NWU-Cu-B and a natural chalcopyrite TC1725 were used as bracketing standards for calibration. Reliable and precise (2SD<0.07‰) δ^{65}Cu values can be obtained using matrix-matched standards under dry plasma condition and calibrated by the standard-sample bracketing method (SSB). However, the δ^{65}Cu values calibrated by non-matrix-matched standards were seriously affected by matrix effect, with a deviation of up to 1.42‰. Therefore, matrix-matched standards are necessary for reliable *in situ* Cu isotope ratio measurement. Although the analytical precision (2SD) is slightly improved, the use of Ga as an internal standard combined with the SSB correction does not reduce the deviation caused by the matrix effect. However, the matrix effect can be significantly suppressed by adding 8.6 μL min^{-1} water into the carrier gas. The matrix-induced δ^{65}Cu deviation of the TC1725 calibrated against the pure copper NWU-Cu-B was reduced from 0.99‰ in dry plasma mode to 0.03‰ in wet plasma mode and achieved a long-term reproducibility of 0.10‰ (2SD). For the Cu isotopic compositions of 12 natural copper-rich minerals determined under wet plasma mode, the deviation of δ^{65}Cu was less than 0.13‰ if the mineral is homogeneous. These results indicate that the non-matrix-matched standardization can be achieved by fs-LA-MC-ICP-MS under wet plasma condition, whether using chalcopyrite or pure copper as the external bracketing standards.

Keywords Cu isotope, *In situ*, Femtosecond laser ablation, Non-matrix-matched calibration

Citation: Lv N, Bao Z, Chen K, Wu K, Yuan H. 2022. Accurate analysis of Cu isotopes by fs-LA-MC-ICP-MS with non-matrix-matched calibration. Science China Earth Sciences, 65(10): 2005–2017, https://doi.org/10.1007/s11430-021-9943-y

1. Introduction

Copper is an important transition metal element with two stable isotopes ^{63}Cu (69.2%) and ^{65}Cu (30.8%). The isotopic ratio is commonly expressed in δ notation (δ^{65}Cu=(R_{sample}/$R_{NIST976}$–1)×1000 where R=^{65}Cu/^{63}Cu). The precise and accurate measurement of ^{65}Cu/^{63}Cu isotope ratios in geological, biological, environmental, and anthropogenic samples has gained increasing attention (Graham et al., 2004; Markl et al., 2006; Jouvin et al., 2012; Lee et al., 2012; Mathur et al., 2012; Aramendía et al., 2013; Ryan et al., 2013; Chiaradia, 2014; Roebbert et al., 2018; Yang et al., 2019). Copper is also a useful tool for studying redox interaction and metal cycling (Moynier et al., 2017). As a metal isotope, copper can directly trace the source of ore-forming metal and the mineralization process (Li et al., 2010; Mathur et al., 2012; Zhao et al., 2017).

Thermal ionization mass spectrometry (TIMS) has previously been used to determine the variation of the Cu isotopes. However, the precision is around 1.5‰ (Shields et al., 1965), which is larger than the terrestrial isotopic variation in most cases. The recent wide application of multi-collectors

* Corresponding author (email: yhlsklcd@126.com, hlyuan@nwu.edu.cn)

inductively coupled plasma mass spectrometry (MC-ICP-MS) makes it possible to determine the copper isotopic composition of geological and biological samples with high precision (0.03–0.07‰) (Borrok et al., 2007; Liu et al., 2014; Hou et al., 2016; Yuan et al., 2017; Sullivan et al., 2020). At present, solution nebulization MC-ICP-MS has been well developed and widely used as the most precise method for Cu isotopes, and significant mass-dependent Cu isotope fractionation can be observed even in high-temperature processes (Graham et al., 2004; Maher and Larson, 2007; Seo et al., 2007; Brzozowski et al., 2020).

For some samples that are fine-grained, complexly intergrown with other minerals or heterogeneous in isotopic composition due to the core-rim structure (Graham et al., 2004; Rouxel et al., 2004; Li et al., 2010), a high spatial resolution analysis is necessary. The laser ablation (LA)-MC-ICP-MS allows us to measure the Cu isotope compositions *in situ* at the resolution of dozens of microns. However, previous research has reported significant isotopic fractionation induced by the laser ablation process. Jackson and Günther (2003) first determined Cu isotope composition using LA-MC-ICP-MS with a high fluence ablation and reported a large deviation (1.5–4.8‰) compared with the ratio analyzed by the solution nebulization MC-ICP-MS. They suggested that the isotopic fractionation was dominated by the preferential volatilization of the lighter Cu isotope and the incomplete ionization of large particles, and the isotope ratios closer to the true value can be achieved by filtering out the large particles from aerosols. Kuhn et al. (2007) reported the small particles produced by a 213 nm laser beam were isotopically lighter by 0.7‰ relative to the large particles. Other research has also described this particle size-related fractionation (d'Abzac et al., 2013; Zhu et al., 2017) and suggests that the femtosecond laser ablation technique would significantly reduce the elemental and isotopic fractionation (Ikehata et al., 2008; Lazarov and Horn, 2015; Zheng et al., 2018; Lin et al., 2019).

In addition, previous research suggests that *in situ* analysis of Cu isotopes using LA-MC-ICP-MS requires a matrix-matched calibration standard to acquire reasonable results. Ikehata et al. (2008) found a severe matrix effect on non-matrix-matched calibration of Cu isotopes using a 780 nm near-infrared femtosecond (NIR-fs) LA-MC-ICP-MS. The offset of Cu isotopic value was found up to 2.67‰ in chalcopyrite, and up to 0.54‰ in chalcocite, when calibrated with the NIST SRM 976. Comparatively, the matrix-matched calibration using 780 nm NIR-fs-LA-MC-ICP-MS can obtain δ^{65}Cu values consistent with the solution value within uncertainty with a precision better than 0.14‰. Ikehata and Hirata (2013) found the δ^{65}Cu shifts over 0.56‰ when using NIR-fs-LA-MC-ICP-MS compared to over 0.76‰ when using 260 nm UV-fs-LA-MC-ICP-MS for cubanite calibrated against NIST SRM 976, suggesting the matrix effect was not significantly reduced by using UV-fs-LA-MC-ICP-MS. Lazarov and Horn (2015) reported that 194 nm UV-fs-LA-MC-ICP-MS analysis did not require matrix-matched reference materials to obtain reliable copper isotope values for many copper-bearing minerals, including sulfides, oxides, and carbonates, and the precision was better than 0.1‰ by using a low laser fluence. Thus, it remains unclear if the accurate non-matrix-matched standardization of copper isotope determination can be directly achieved by UV-fs-LA-MC-ICP-MS in practice.

To broaden the application of the femtosecond laser system and reduce the matrix effect, some researchers introduced water into the carrier gas. This so-called water-assisted technique or "wet plasma" has been found to significantly suppressed the matrix effect and the mass load effect (Oeser et al., 2014; Allner et al., 2017; Luo et al., 2018; Zheng et al., 2018; Lin et al., 2019). Zheng et al. (2018) evaluated the matrix effect during Fe isotope analysis using ns-LA-MC-ICP-MS and fs-LA-MC-ICP-MS and suggested that the accuracy of isotope ratios during the non-matrix-matched determination under a "dry" condition have been significantly improved by water addition. Lin et al. (2019) reported the precise Li isotope determination of tourmalines using NIST glass as non-matrix-matched standards, and the matrix effects of both ns-LA-MC-ICP-MS and fs-LA-MC-ICP-MS were significantly reduced by adding water. The deviation (~1.5‰) of δ^{7}Li using fs-LA-MC-ICP-MS under a "dry plasma" condition has been basically eliminated during the water-assisted ablation process. In fact, the accurate *in situ* isotope determination by LA-MC-ICP-MS in many studies has been performed under the "wet plasma" condition (Oeser et al., 2014; Schuessler and von Blanckenburg, 2014; Lazarov and Horn, 2015).

In this study, we evaluated the matrix effect of the *in situ* method for determining the Cu isotope compositions of 12 common copper-bearing minerals using 206 nm ultraviolet fs-LA-MC-ICP-MS via matrix-matched and non-matrix-matched standardization. In addition, water aerosol, nitrogen, and internal standard Ga were added to the plasma to investigate the influence of matrix effect during laser ablation Cu isotope analysis. Under the condition that the matrix-matched determination is hard to process, this study seeks to provide an alternative method for Cu isotope determination in worldwide laboratories.

2. Experimental procedures

2.1 Instruments and data acquisition

The Cu isotope measurements were conducted on a Neptune Plus MC-ICP-MS (Thermo Fisher Scientific, Germany) in combination with an NWR-Femto^{UC} Dualwave femtosecond laser ablation system (ESI, USA) at the State Key Laboratory

of Continental Dynamics (SKLCD), Northwest University, China. The femtosecond laser system was equipped with a fundamental near-infrared wavelength (1028 nm) and operated in ultraviolet wavelength 257 nm by the fourth-harmonic generation and wavelength 206 nm by the fifth-harmonic generation. A six-inch (1 inch=2.54 cm) TV2 chamber was equipped for the laser ablation system. The chamber has been inserted a Floating Floor, where the shape and the size of the sample mounts would not be strictly limited. The samples can be placed at any position in the sample chamber drawer using plasticine. The Neptune Plus MC-ICP-MS was equipped with 9 moveable Faraday cups and seven ion counters. ^{63}Cu, ^{65}Cu, ^{69}Ga, and ^{70}Ga were simultaneously measured in 10^{11} Ω resistor Faraday cups L4, L2, H2, and H3, respectively. NIST SRM 994 Ga (^{69}Ga/^{71}Ga=1.50676 ±0.00039 (Machlan et al., 1986)) was used for the instrumental mass bias correction. The NIST SRM 994 metal is dissolve and dilute to 100 μg g^{-1} solution in 2% HNO_3. The parameters of the instrument are always tuned to reach the highest sensitivity during "dry" and "wet" plasma condition, and the detailed instrument settings and operating parameters are listed in Table 1. For all the minerals, line-scan ablations were performed with a spot diameter of 10–30 μm and a line length of ~60 μm. Due to the different concentrations of Cu in mineral samples, the spot size was varied to provide near-constant Cu signal intensity between samples and bracketing standards. The signal intensity of ^{63}Cu ranged from 5 V to 15 V on 10^{11} Ω resistors during the MC-ICP-MS analysis. Due to the different Cu content in copper-rich minerals, the signal intensities of the natural mineral samples were pre-analyzed, and then the ablation spot size was adjusted to ensure that the signal intensity of samples and the reference materials matched with each other by ±15%. The signal intensity of aspirated NIST SRM 994 Ga was always adjusted to be within ±20% relative to the signal intensity of Cu by changing the concentration of Ga in ultra-pure water. Each measurement consists of 30 s background, 52.4 s data acquisition, and 60 s washout. The on-peak baseline was measured with the aspirated water and NIST SRM 994 Ga before the laser emission in wet plasma condition. The background of ^{63}Cu was less than 5 mV in both dry and wet ablation modes. All the samples and standards were analyzed using line-scan ablation to get a relatively stable signal and a lower effect of down hole fractionation. The scanning speed was set to 1 μm s^{-1}, and a total of 100 cycles of data can be obtained for calculation during the whole 52.4 s measurement time. The samples and bracketing standards were placed close to each other. Generally, the standards and the samples are placed parallel to the horizontal direction, and the bracketing standard is placed on the left or right of the

Table 1 Summary of the operation parameters of fs-LA-MC-ICP-MS for Cu isotope measurements

MC-ICP-MS	Neptune Plus (Thermo Fisher)
RF power	1200 W
Cooling gas flow rate (Ar)	~15.0 L min^{-1}
Auxiliary gas flow rate (Ar)	~0.70 L min^{-1}
Sample gas flow rate (Ar)	1.05 L min^{-1} (dry plasma); 0.72 L min^{-1} (wet plasma)
Add gas flow rate (Ar)	0.00 L min^{-1} (dry plasma); 0.30 L min^{-1} (wet plasma)
Block number	1
Cycle number	100
Integration time	0.524 s
Guard Electrode (GE)	On
Analysis mode	Static
Nebulizer	PFA micro-flow
Sample uptake	~50 μL min^{-1}
Interface cones	Nickel, standard sample cone + H skimmer cone
Laser ablation system	NWR-Femto^{UC}
Wavelength	206 nm
Pulse duration	190 fs
Laser beam spatial intensity profile	Gaussian distribution
Energy density	0.50 J cm^{-2}
Frequency	8 Hz
Spot size	10–30 μm
Line scanning rate	1 μm s^{-1}
Helium carrier gas flow rate	700–750 mL min^{-1} (dry plasma); 600–650 mL min^{-1} (wet plasma)

sample with no gap in the middle during measurement, so that the position effect inside the sample cell can be ignored within the uncertainty. All the Cu isotope ratios were reported in the delta notation for the $^{65}Cu/^{63}Cu$ ($\delta^{65}Cu$) relative to NIST SRM 976:

$$\delta^{65}Cu_{std} = \left(\frac{\left(\frac{^{65}Cu}{^{63}Cu}\right)_{sam}}{\left(\frac{^{65}Cu}{^{63}Cu}\right)_{std}} - 1 \right) \times 1000, \quad (1)$$

$$\delta^{65}Cu_{NIST\ SRM\ 976} = \delta_{sam}{}^{65}Cu_{std} + \delta_{std}{}^{65}Cu_{NIST\ SRM\ 976} + \delta_{sam}{}^{65}Cu_{std} \times \delta_{std}{}^{65}Cu_{NIST\ SRM\ 976} \times 10^{-3}, \quad (2)$$

where $\delta_a{}^{65}Cu_b$ is the per mileage deviation of sample a relative to standard b, the subscripts std and sam represent the bracketing standards (NWU-Cu-A or TC1725) and samples used in this study. The external precision of the average measurement is expressed as 2SD, and the internal precision of a single analysis is expressed as 2SE, defined as follows:

$$2SE = 2 \times \sqrt{\left(\frac{\sigma Cu_{std1}}{Cu_{std1}}\right)^2 + \left(\frac{\sigma Cu_{sam}}{Cu_{sam}}\right)^2 + \left(\frac{\sigma Cu_{std2}}{Cu_{std2}}\right)^2}, \quad (3)$$

where σCu_{std1} is the standard error of the first bracketing standard, and σCu_{std2} is the standard error of the second bracketing standard, σCu_{sam} represents the standard error of the sample, Cu_{std1} is the $^{65}Cu/^{63}Cu$ value of the first bracketing standard, and Cu_{std2} is the $^{65}Cu/^{63}Cu$ value of the second bracketing standard.

2.2 Connecting laser system and MC-ICP-MS

Helium gas was used as a carrier gas to flush the sample cell during the laser ablation. In dry plasma condition, the ablated material flushed out from the sample cell by helium was then mixed with argon (sample gas) by a homemade glass homogenizer to obtain stable transportation (Figure 1). The sample aerosols carried by the Ar-He gas mixture were subsequently introduced into the ICP. During wet plasma condition, ultra-pure water was introduced into the ICP through a quartz glass spray chamber and a PFA MicroFlow nebulizer (~50 μL min^{-1}) using the stream of argon gas (added gas). The internal standard NIST SRM 994 Ga solution was added into the ultra-pure water and introduced to be mixed with sample aerosols. The NIST SRM 994 Ga and water were added to sample aerosols just before the ICP torch using a "Y" connector. The water uptake rate was controlled by adjusting the flow rate of nebulization argon gas using a mass flow controller on the MC-ICP-MS. Because the nebulization argon flow rate was very low during our laser ablation analysis, the uptake rate of the nebulizer is lower than its nominal rate. In addition, part of the water aerosol will condense in the spray chamber and be discharged as waste. Thus, the actual uptake rates were determined by measuring the mass loss of the solution and the weight of the waste after aspiration for a known period. The additional stream of nitrogen was first mixed with argon (sample gas), via a "Y" connector and then mixed with the carrier gas in the glass homogenizer (Figure 1).

2.3 Sample preparation

This study examined the Cu isotopic compositions of 12 copper-bearing minerals, including a native copper (Cu), five natural copper sulfides (chalcopyrite ($CuFeS_2$), digenite ($4Cu_2S{\cdot}CuS$), covellite (CuS), tetrahedrite ($(Cu, Fe)_{12}Sb_4S_{13}$), bornite (Cu_5FeS_4)), two copper carbonates (azurite ($Cu_3(CO_3)_2(OH)_2$), malachite ($Cu_2CO_3(OH)_2$)), one copper oxide (cuprite (Cu_2O)) and one copper chloride (atacamite ($Cu_2(OH)_3Cl$)). The major and minor elements analyzed by an electron probe microanalyser (EPMA: JEOL JXA-8230) at the SKLCD are summarized in Table 2.

The pure copper NWU-Cu-B and the in-house natural chalcopyrite reference TC1725 were applied as the *in situ* bracketing standards to study the matrix-matched and the non-matrix-matched calibration of copper-bearing minerals. NWU-Cu-B and TC1725 are considered isotopically homogeneous for Cu isotope compositions and their $\delta^{65}Cu$ values relative to NIST SRM 976 are –0.05±0.03‰ (2SD) (Yuan et al., 2017) and –0.06±0.03‰ (2SD) (Bao et al., 2021), respectively. Fragments of the reference materials and copper minerals were mounted in 16 mm-diameter round epoxy mounts and polished with one-micron diamond paper to obtain flat surfaces. Due to the heterogeneous distribution of copper isotopes in natural copper minerals, a micro-drilling system (MSS VI, Relion Industries, USA) was applied to extract sample powders on the surface of the target sample, and the Cu isotopes of the minerals were measured using solution nebulization MC-ICP-MS as described by Lv et al. (2020). The diameter of the microdrill sampling pit was 300–350 μm, and the line-scan ablation analyses were processed around the edge of the microdrill sampling pit.

3. Results and discussion

3.1 Effects of laser fluence and frequency

The measurement of isotopic ratios may be affected by the parameters of laser ablation system, including pulse duration, wavelength, energy density, and the frequency of the laser beam, resulting in isotopic fractionation(Hirayama and Obara, 2005; Lazarov and Horn, 2015). This study designed an experiment to test the effects of laser fluence and frequency on Cu isotope analysis. A SSB protocol was used to analyze chalcopyrite and pure copper, respectively, under different laser fluences. To avoid the potential matrix effect,

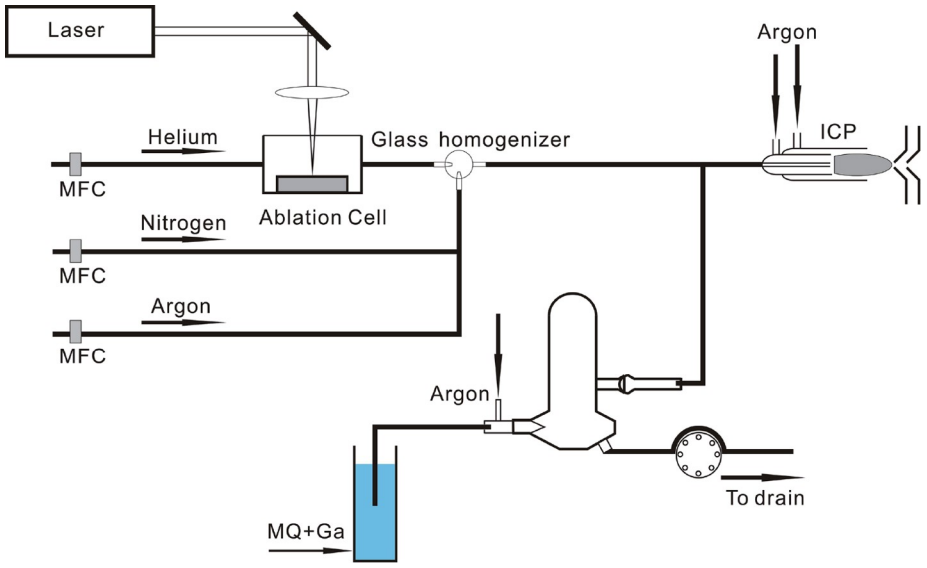

Figure 1 Schematic representation of the online addition of water and Ga standard solution to the plasma during laser ablation.

Table 2 Mass fraction of major and minor elements of samples in this study[a)]

Sample species	Sample name	Species	Formula	Cu concentration (wt%)	Other elements (wt%)
Simple substance	NC	Native copper	Cu	99.26	
Sulfide	CPY-1	Chalcopyrite	$CuFeS_2$	34.44	S-34.88, Fe-30.38
	CPY-SG	Chalcopyrite	$CuFeS_2$	34.85	S-34.90, Fe-30.13, Co-0.09
	DIG	Digenite	$4Cu_2S{\cdot}CuS$	78.83	S-21.55
	COV	Covellite	CuS	67.18	S-32.89
	TET-G	Tetrahedrite	$(Cu, Fe)_{12}Sb_4S_{13}$	41.42	S-25.93, Sb-17.84, As-8.13, Fe-4.87, Zn-1.94, Ag-0.10
	TC1725	Chalcopyrite	$CuFeS_2$	33.78[b)]	Fe-30.96[b)]
	BOR-Q	Bornite	Cu_5FeS_4	34.32	S-35.38, Fe-30.21
Carbonate	AZU	Azurite	$Cu_3(CO_3)_2(OH)_2$	49.83	
	MAL-1	Malachite	$Cu_2CO_3(OH)_2$	57.22	
	MAL-2	Malachite	$Cu_2CO_3(OH)_2$	54.98	Zn-0.08
Oxide	CUP-G	Cuprite	Cu_2O	85.49	
Chloride	ATA-SG	Atacamite	$Cu_2(OH)_3Cl$	49.50	Zn-0.10

a) Elements containing less than 0.05 wt% are not listed; b) Bao et al., 2021.

chalcopyrite was calibrated by TC1725 and pure copper was calibrated by NWU-Cu-B. The δ^{65}Cu value was determined by varying the laser energy densities from 0.5 to 2.5 J cm^{-2}, while the laser frequency and the linear scanning speed were fixed at 8 Hz and 1 μm s^{-1}, the standards were analyzed under the same laser ablation parameters as the corresponding samples. For each energy density, the Cu isotope ratios were analyzed four times, and the mean δ^{65}Cu values are summarized in Figure 2. With the increase of the energy density, the mean δ^{65}Cu of both pure copper and chalcopyrite are consistent with their respective solution values. However, the higher laser fluences (>1 J cm^{-2}) led to worse precision (2SD) and reproducibility. The precision (2SD) of chalcopyrite CPY-1 was up to 0.15‰ when applying an energy density of 2.5 J cm^{-2}. Thus, a low laser fluence (<1 J cm^{-2}) is preferential for LA-MC-ICP-MS Cu isotope analysis (Lv, 2021).

The effect of laser frequency was evaluated by determining the δ^{65}Cu values of chalcopyrite and pure copper using varying frequencies from 2 to 20 Hz. Other laser parameters were fixed at 0.5 J cm^{-2} for laser fluence and 1 μm s^{-1} for linear scanning speed. The Cu isotope ratios were analyzed four times for each laser frequency and the mean δ^{65}Cu values are summarized in Figure 3. The δ^{65}Cu of chalcopyrite tends to be lighter with the increase of frequency (Figure 3a). When the frequency is less than 4 Hz, the δ^{65}Cu tends to be heavier relative to the solution value, but when the frequency is higher than 15 Hz, the δ^{65}Cu tends to be lighter relative to

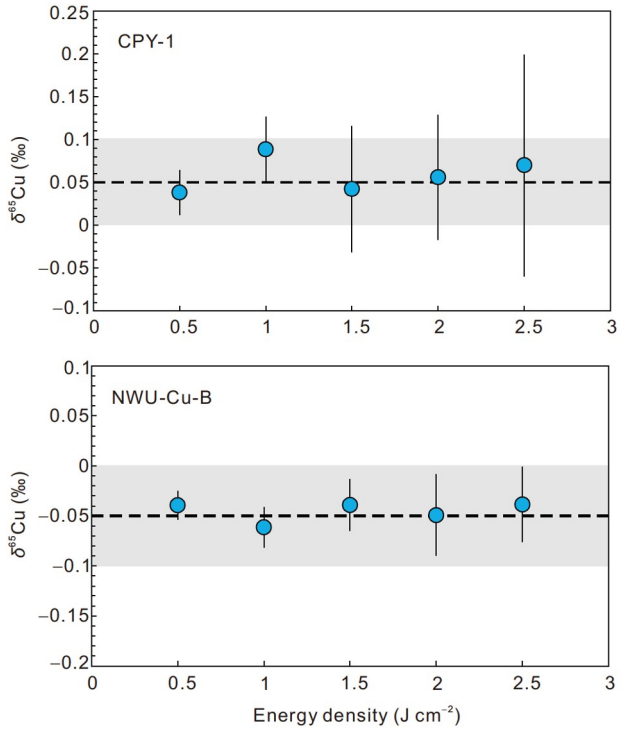

Figure 2 Variations of the δ^{65}Cu values measured for chalcopyrite (CPY-1) and pure copper (NWU-Cu-B) with the different laser energy densities. Error bars are 2SD, calculated based on four repeated measurements. The grey-shaded horizontal field in each plot represents a 0.05‰ deviation.

the solution reference value. Though the effect of laser frequency seems absent on pure copper using frequencies ranging from 2 to 20 Hz, the δ^{65}Cu value is relatively lower using frequency ≤4 Hz (Figure 3b). Using frequencies between 6 Hz and 10 Hz can acquire δ^{65}Cu value that is consistent with the solution value within the 0.05‰ uncertainty (Lv, 2021). Therefore, in the subsequent experiments, the laser fluence of 0.5 J cm^{-2} and the frequency of 8 Hz were applied to ensure that the laser-induced isotope fractionation can be ignored during the *in situ* Cu isotope analysis.

3.2 Effect of signal intensity

The concentration mismatch between the samples and the standards can cause significant deviation during isotope measurement using solution nebulization MC-ICP-MS. This effect of concentration induced the matrix effect, which leads to a difference in the mass bias of MC-ICP-MS (Zhu et al., 2002). This study systematically evaluated the effects of mismatched signal intensities of samples and standards during the determination of copper isotope using LA-MC-ICP-MS. The parameters of laser ablation were set at 0.5 J cm^{-2}, 8 Hz and 1 μm s^{-1}, while the in-house standard CPY-1 was calibrated using TC1725 as the matrix-matched bracketing standard. The ^{63}Cu signal intensity of TC1725 was fixed at 6 V, and the ^{63}Cu signal intensities of samples ranged from 2 to 12 V by changing the spot size of the laser beam. As illustrated in Figure 4, operation under the mismatched signal intensity of the bracketing sequence will result in a severe deviation of the δ^{65}Cu value. When the ^{63}Cu signal intensity of the bracketing standard is about 6 V and the sample signal is about 2 V (the signal intensity of the sample is 66.7% lower than that of the standard), the δ^{65}Cu of chalcopyrite CPY-1 is 0.26‰ lighter than its solution value. When the signal intensity of the sample is twice as high as the standard signal (the ^{63}Cu signal intensity of samples is about 12 V), the δ^{65}Cu of chalcopyrite is 0.20‰ heavier than the solution value. However, when the ^{63}Cu signal intensity of the sample is range from 5 to 7 V (±15% relative to the 6 V signal intensity of standard), the δ^{65}Cu of chalcopyrite agrees with the solution value within the uncertainty. Therefore, it is necessary to strictly match the signal intensities of the samples and the bracketing standards for Cu isotope determination using laser ablation MC-ICP-MS (Lv, 2021). For the non-matrix-matched standardization, the signal intensities of unknown samples should be pre-tested due to the signal sensitivity of different minerals varies significantly. By changing the ablation spots size, the Cu signal of samples and standards should be controlled within ±15% relative to each other using the SSB protocol.

3.3 Matrix effect of Cu isotope analysis using fs-LA-MC-ICP-MS (dry plasma)

The δ^{65}Cu values of 12 natural copper minerals were analyzed by fs-LA-MC-ICP-MS with pure copper NWU-Cu-B and chalcopyrite TC1725 as bracketing standards. Each sample was repeatedly analyzed (n=6) by line-scan mode, and the results were compared with the solution values obtained using the microdrilling technique. The results were summarized in Figure 5 and Table 3. The δ^{65}Cu values of natural minerals with different matrices calibrated against NWU-Cu-B using 206 nm femtosecond laser ablation system are systematically higher than the solution nebulization values, indicating the measurement of non-matrix-matched Cu isotopic composition was strongly affected by the matrix effect using 206 nm UV-fs-LA-MC-ICP-MS.

The δ^{65}Cu values of copper sulfides (chalcopyrite CPY-1, CPY-SG, digenite DIG, covellite COV, tetrahedrite TET-G, bornite BOR-Q) calibrated against pure copper NWU-Cu-B show deviations of 0.73–1.10‰ from their solution values (Figure 5, Table 3). The δ^{65}Cu values of carbonates (azurite AZU, malachite, MAL-1, MAL-2) calibrated against pure copper have deviations of 0.58–0.94‰ from the solution values. The mean δ^{65}Cu values of cuprite CUP-G and atacamite ATA-SG corrected by NWU-Cu-B is 0.78‰ and 0.85‰, higher than their solution values. In contrast, the mean δ^{65}Cu value of natural copper NC (0.31±0.06‰, 2SD, n=6) obtained by laser ablation experiments using pure

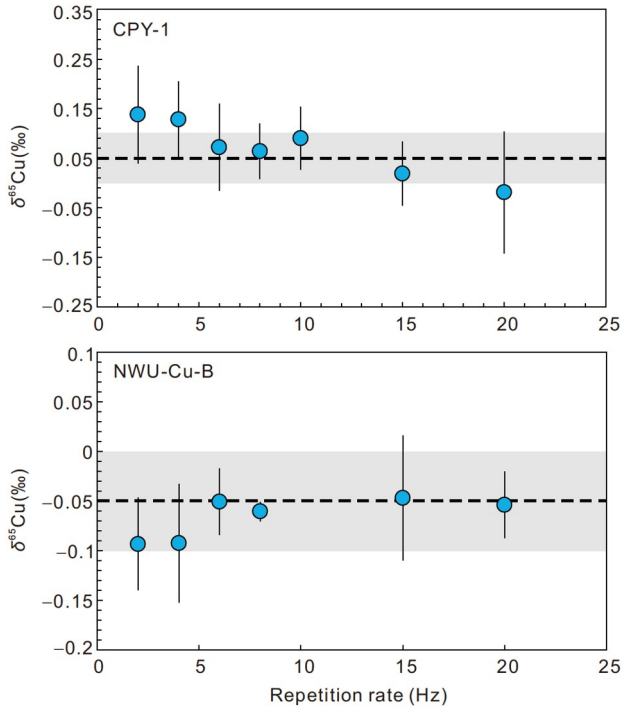

Figure 3 Variations of the δ^{65}Cu values measured for chalcopyrite (CPY-1) and pure copper (NWU-Cu-B) with the different laser frequencies. Error bars are 2SD, calculated based on four repeated measurements. The grey-shaded horizontal field in each plot represents a 0.05‰ deviation.

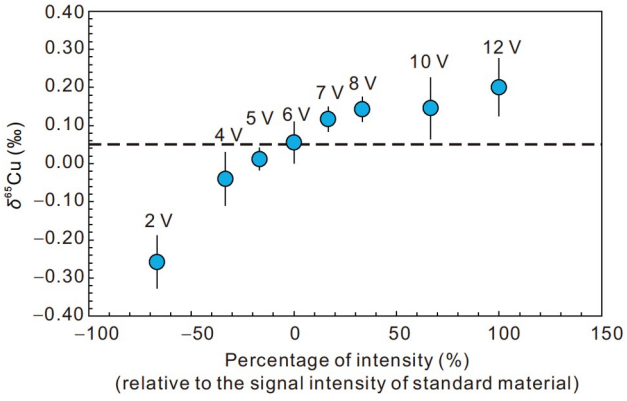

Figure 4 The δ^{65}Cu values of chalcopyrite CPY-1 using the mismatched signal intensity of standards and samples. The signal intensity of TC1725 was fixed at 6 V, and the signal intensity of sample CPY-1 ranged from 2 to 12 V. The abscissa is the percentage of relative deviation of signal intensity between standards and samples. The dotted line is the solution value of CPY-1 (0.05±0.02‰). Error bars are 2SD of four repeated measurements.

copper as the bracketing standard agrees well with the solution nebulization value (δ^{65}Cu=0.23±0.02‰, 2SD, n=4).

The 12 natural minerals were also analyzed using chalcopyrite TC1725 as the bracketing standard. Except for tetrahedrite TET-G, the mean δ^{65}Cu values of copper sulfides (chalcopyrite CPY-1, CPY-SG, digenite DIG, covellite COV, bornite BOR-Q) were all in good agreement with their solution values, the deviation was less than 0.07‰ (Table 3). Though both TC1725 and TET-G are sulfides, the mean δ^{65}Cu value of tetrahedrite calibrated against TC1725 is 0.14‰ lighter than its solution value. This may be attributed to the 17.84 wt% Sb contained in TET-G (Table 2), which results in a matrix effect. The laser ablation analysis on oxide (cuprite CUP-G) and chloride (atacamite ATA-SG) calibrate by TC1725 yield the mean δ^{65}Cu values of 2.08±0.18‰ (2SD, n=6) and 1.50±0.18‰ (2SD, n=6) respectively, both of which are in good agreement with the solution values of 2.03±0.18‰ (2SD, n=6) for CUP-G and 1.51±0.18‰ (2SD, n=6) for ATA-SG. The results indicate that the Cu isotope compositions of cuprite and atacamite can be calibrated by chalcopyrite using 206 nm fs-LA-MC-ICP-MS. In contrast, the mean δ^{65}Cu values of carbonate (azurite AZU, malachite, MAL-1, MAL-2) calibrated by chalcopyrite were 0.22–0.26‰ lighter than the solution values, and up to 1.42‰ deviation of δ^{65}Cu values was found for native copper (NC) using chalcopyrite TC1725 as the bracketing standard.

The results clearly showed that, for copper-rich minerals, Cu isotope determination using 206 nm UV-fs-LA-MC-ICP-MS and calibrated using pure copper (NWU-Cu-B) as the bracketing standard suffered from severe matrix effect and up to 1.42‰ systematical error was found during the non-matrix-matched standardization. For laser ablation Cu isotope determination using chalcopyrite (TC1725) as the bracketing standard, most copper sulfides (except tetrahedrite), cuprite and atacamite give consistent results within uncertainty with the solution values. However, for laser experiment of copper carbonate calibrated by TC1725 still causes systematic bias compared with solution values. This indicates that for 206 nm UV-fs-LA-MC-ICP-MS analysis, matrix-matched standardization is still necessary (Lv, 2021). Reliable Cu isotope compositions can only be obtained by calibrating against matrix-matched standards or the standards with similar chemical compositions. However, the matrix-matched standard of Cu isotopes is very rare. As far as we know, there is only one published Cu isotopic standard of natural minerals (TC1725, chalcopyrite). The lack of reference materials greatly limits the application of the *in situ* Cu isotope analysis. In this study, we try to determine the Cu isotope of cooper-bearing minerals with non-matrix-matched standardization and hope to provide an alternative method for Cu isotopes determination in other laboratories worldwide.

3.4 Non-matrix-matched calibration of Cu isotope analysis under wet plasma condition

The severe matrix effect greatly limits the application of laser ablation Cu isotopic analytical technique. To achieve accurate non-matrix-matched standardization, a small amount of water was introduced into the plasma. The Cu isotope analysis of 12 natural copper minerals was conducted under the so-called “wet” plasma condition. After adding

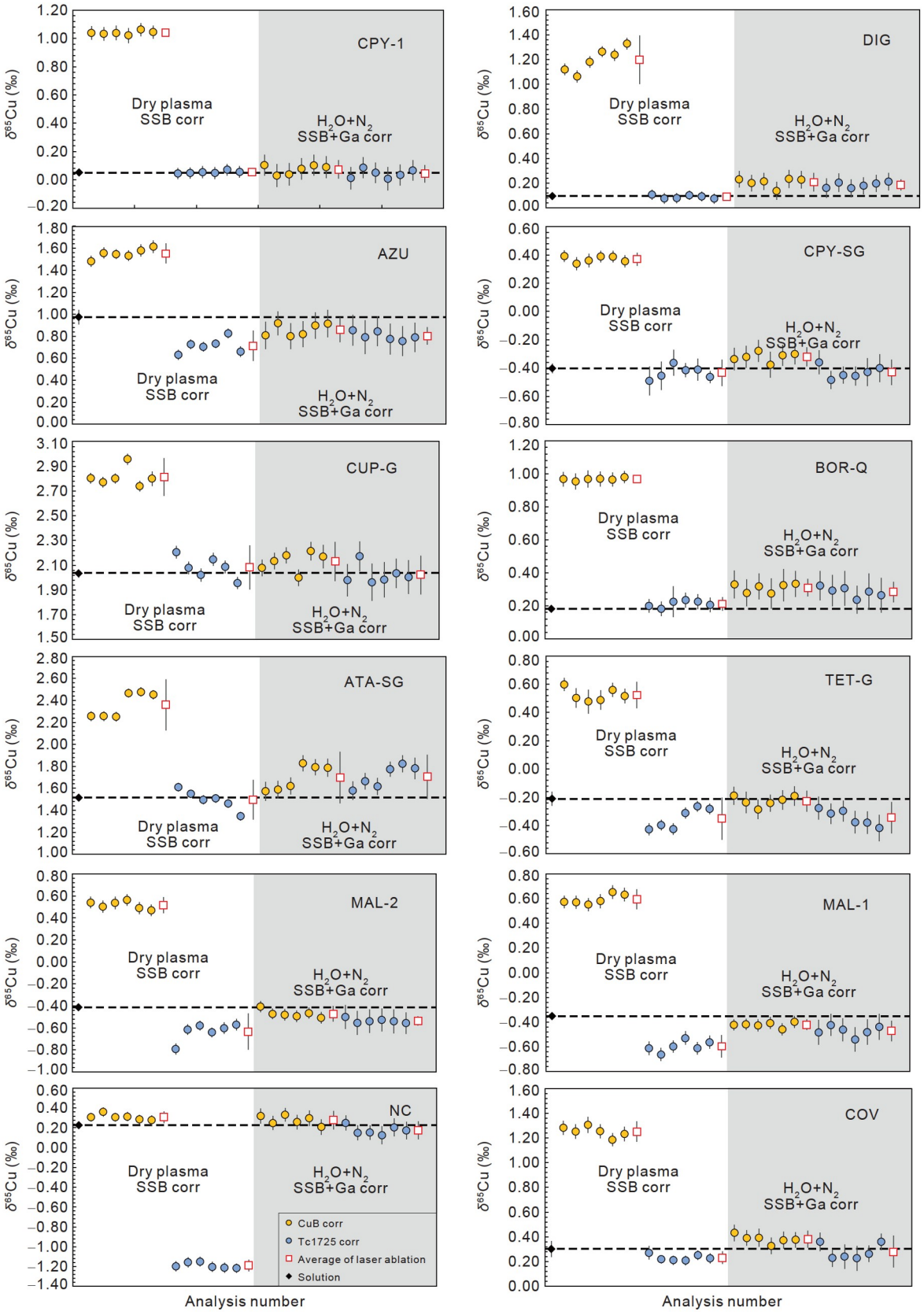

Figure 5 δ^{65}Cu values of copper-bearing minerals measured by laser ablation and solution. Laser ablation analyses were processed under dry plasma condition (white area) and wet plasma condition (grey area). All the δ^{65}Cu values were calibrated by the SSB protocol under dry plasma condition and calibrated by the SSB combined with Ga internal standard under wet plasma condition. Error bars are 2SE for single analyses and 2SD for average values.

Table 3 Laser ablation and solution measurement of copper-bearing minerals

Sample	MC-ICP-MS (SSB+Ga)[a]			fs-LA-MC-ICP-MS (SSB) Dry plasma[b]								fs-LA-MC-ICP-MS (SSB+Ga) Adding 8.6 μL min^{-1} water+2 mL min^{-1} N_2[c]							
				TC1725 corr[d]				CUB corr[e]				TC1725 corr[d]				CUB corr[e]			
	δ^{65}Cu (‰)	2SD	*n*	δ^{65}Cu (‰)	2SD	*n*	offset	δ^{65}Cu (‰)	2SD	*n*	offset	δ^{65}Cu (‰)	2SD	*n*	offset	δ^{65}Cu (‰)	2SD	*n*	offset
NC	0.23	0.02	4	–1.19	0.06	6	–1.42	0.31	0.06	6	0.08	0.18	0.09	6	–0.05	0.28	0.09	6	0.05
CPY-1	0.05	0.02	4	0.05	0.02	6	0.01	1.04	0.03	6	0.99	0.04	0.06	6	–0.01	0.07	0.06	6	0.03
CPY-SG	–0.40	0.03	3	–0.43	0.09	6	–0.03	0.37	0.04	6	0.77	–0.43	0.09	6	–0.03	–0.32	0.07	6	0.08
DIG	0.10	0.03	4	0.09	0.03	6	–0.01	1.20	0.20	6	1.10	0.19	0.04	6	0.09	0.21	0.07	6	0.11
COV	0.30	0.06	4	0.23	0.06	6	–0.07	1.25	0.08	6	0.95	0.28	0.13	6	–0.02	0.38	0.07	6	0.08
TET-G	–0.21	0.05	3	–0.35	0.15	6	–0.14	0.52	0.09	6	0.73	–0.34	0.11	6	–0.13	–0.24	0.07	6	–0.03
BOR-Q	0.18	0.01	3	0.21	0.04	6	0.03	0.97	0.02	6	0.79	0.28	0.06	6	0.10	0.31	0.05	6	0.13
AZU	0.98	0.06	4	0.71	0.14	6	–0.26	1.55	0.09	6	0.58	0.80	0.08	6	–0.17	0.86	0.11	6	–0.12
MAL-1	–0.35	0.02	4	–0.60	0.09	6	–0.24	0.59	0.08	6	0.94	–0.47	0.08	6	–0.12	–0.42	0.04	6	–0.07
MAL-2	–0.41	0.02	4	–0.63	0.16	6	–0.22	0.52	0.07	6	0.93	–0.54	0.04	6	–0.12	–0.47	0.07	6	–0.06
CUP-G	2.03	0.03	3	2.08	0.18	6	0.05	2.81	0.15	6	0.78	2.02	0.16	6	–0.01	2.13	0.16	6	0.10
ATA-SG	1.51	0.03	3	1.50	0.18	6	–0.02	2.36	0.23	6	0.85	1.71	0.20	6	0.19	1.77	0.23	6	0.25
TC1725	–0.06	0.03						0.93	0.04	6	0.99					–0.09	0.04	6	–0.03

a) Reference value obtained using microdrill and solution nebulization MC-ICP-MS; b) laser analyses under dry plasma condition and SSB protocol; c) adding 8.6 μL min^{-1} water and 2 mL min^{-1} N_2 into carrier gas, calibrated using SSB combine with Ga as internal standard; d) calibrate using TC1725; e) calibrate using NWU-Cu-B; *n* represent the number of analysis, offset represent the deviation of δ^{65}Cu (‰) relative to the solution value.

ultra-pure water into the plasma, the signal intensity of ^{63}Cu was decreased by ~28% (the introduced amount of water was about 8.6 μL min^{-1}) relative to those measured under dry plasma condition during the same analytical session (Appendix Figure S1, https://link.springer.com). Such a decrease is consistent with previous studies (Zheng et al., 2018; Lin et al., 2019). NIST SRM 994 Ga was added in the ultrapure water as an internal standard to calibrate the mass bias of the instrument. The signal intensity of Ga was adjusted by changing the concentration of Ga in ultrapure water to match the signal intensity of Cu within ±20%. In addition, 2 mL min^{-1} nitrogen was simultaneously introduced into the plasma to reduce the yield of oxide and hydride (Hill et al., 1992; Hu et al., 2008; Fu et al., 2016), and the signal intensity of ^{63}Cu was reduced again by about 63% relative to those adding water aerosol (8.6 μL min^{-1}) (Figure S1). However, the results show the use of Ga as an internal standard has little effect on the matrix effect (Figure 6). The δ^{65}Cu values before and after internal standard correction are basically the same, but the precision (2SD) of the mean δ^{65}Cu values after Ga correction are better than those of the SSB correction only.

The accuracy and precision of matrix-matched calibration of δ^{65}Cu are not significantly improved by introducing water. For matrix-matched calibration with the chalcopyrite TC1725, the deviations of δ^{65}Cu values relative to solution value are 0.02‰ for CPY-1, –0.03‰ for CPY-SG, –0.07‰ for COV, and –0.01‰ for DIG in dry plasma condition, while the deviations are 0.01‰ for CPY-1, –0.03‰ for CPY-SG, –0.02‰ for COV, and 0.09‰ for DIG in wet plasma condition. The mean δ^{65}Cu value of NC obtained using NWU-Cu-B as matrix-matched reference is 0.08‰ deviated from the solution value under dry plasma condition and 0.05‰ deviated from the solution value under wet plasma condition.

However, the introduction of water can significantly improve the results obtained from non-matrix-matched calibration. The mean δ^{65}Cu values of copper sulfides (chalcopyrite CPY-1, CPY-SG, digenite DIG, covellite COV, bornite BOR-Q) calibrated against the NWU-Cu-B are in good agreement with their solution values, the deviations range from 0.03‰ to 0.13‰ (Figure 5; Table 3). For copper carbonates (azurite AZU, malachite, MAL-1, MAL-2), the deviations of mean δ^{65}Cu values range from 0.06‰ to 0.12‰. The laser ablation analyses on oxide (cuprite CUP-G) and chloride (atacamite ATA-SG) yield mean δ^{65}Cu values that are 0.10‰ and 0.25‰ deviated from the solution values, respectively (Figure 5; Table 3). These results indicate that the introduction of water can significantly reduce the matrix effect when using pure copper to calibrate the copper-bearing minerals. Except for the deviation of atacamite (ATA-SG) and azurite (AZU) are slightly larger due to their extreme heterogeneity, the δ^{65}Cu values obtained by laser ablation of the rest of the samples are close to those of solution values.

For samples with a systematic deviation of δ^{65}Cu due to the matrix effect calibrated by TC1725 under dry plasma condition, the mean δ^{65}Cu values are also in good agreement with solution values under wet plasma condition. The mean δ^{65}Cu values of carbonates AZU, MAL-1, MAL-2 and nat-

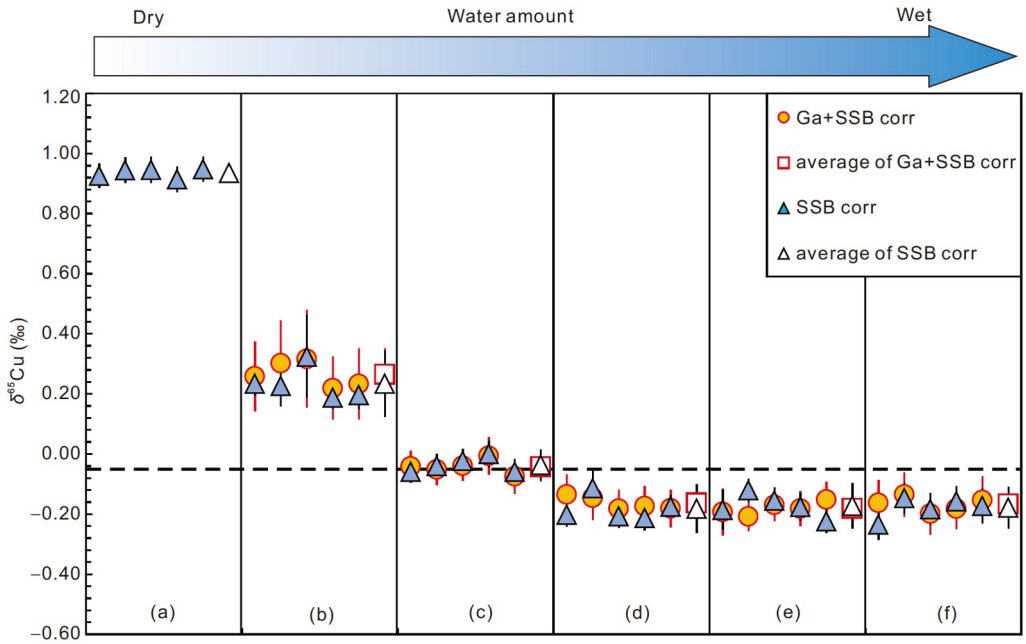

Figure 6 δ^{65}Cu of TC1725 non-matrix-matched calibrated using NWU-Cu-B under varied water introducing rates. SSB corr represents the results calibrated using the SSB protocol; Ga+SSB corr represents the results calibrated using the SSB combined with Ga as internal standard; the dotted line is the preferred value of TC1725. Error bars for single analysis are 2SE, for average values are 2SD. The water introducing rate increases from (a) to (f), (a) dry plasma condition; (b) 0.2 L min^{-1} added gas (water introducing rate ~6.5 μL min^{-1}); (c) 0.3 L min^{-1} added gas (water introducing rate ~8.6 μL min^{-1}); (d) 0.4 L min^{-1} added gas (water introducing rate ~14.5 μL min^{-1}); (e) 0.5 L min^{-1} added gas (water introducing rate ~19.1 μL min^{-1}); (f) 0.7 L min^{-1} added gas (water introducing rate ~30.5 μL min^{-1}).

ural copper NC calibrated against the TC1725 are –0.17‰, –0.12‰, –0.12‰ and –0.05‰ deviated from the solution values, respectively. All the above results indicate that the matrix effect of non-matrix-matched standardization using chalcopyrite as bracketing standard has also been significantly reduced under wet plasma condition. Among them, the results of carbonate calibrated by pure copper are better than that of calibration using chalcopyrite after adding water. The results of tetrahedrite (TET-G) corrected by TC1725 has no obvious improvement in wet plasma, while the results calibrated against pure copper are closer to its solution value with a mean δ^{65}Cu value deviation of –0.03‰ within uncertainty (Figure 5; Table 3). However, due to the reduction of signal intensity resulted from the introduction of water and nitrogen, the precision (2SE) of the single analysis calibrated using the SSB combined with Ga as the internal standard under wet plasma condition is worse than those under dry plasma and calibrated using the SSB protocol (Figure 5). Under dry plasma condition, the internal precision (2SE) of CPY-1 calibrated against TC1725 or NWU-Cu-B using the SSB protocol is less than 0.05‰, while the precision increases to 0.08‰ after adding water and nitrogen.

In order to further confirm the contribution to the suppression of the matrix effect between Ga and water introduction on the matrix effect, only ultrapure water was introduced to the ICP, and the sample DIG, which is considered to be relatively homogeneous in δ^{65}Cu, was calibrated by pure copper NWU-Cu-B and chalcopyrite TC1725 using SSB method. The results showed that the introduction of water is the main factor in suppressing the matrix effect. The mean δ^{65}Cu value of DIG is 0.20±0.08‰ (2SD, n=3) for pure copper calibration and 0.14±0.10‰ (2SD, n=3) for chalcopyrite calibration (Figure S2), which is consistent with the results of introducing water and Ga solution at the same time (Table 3). Furthermore, during the solution nebulizer MC-ICP-MS analysis, the δ^{65}Cu value of NWU-Cu-A with additional matrix elements is consistent with that of pure copper solution using SSB calibration without adding internal standard Ga (Table 4). Therefore, the matrix effect can be significantly reduced under wet plasma condition, whether Ga solution is introduced or not. However, the precision of the result after Ga correction is improved (Table 3).

In addition, to match the signal intensity of Ga with Cu during the water amount experiments, the smaller the water aerosol is introduced, the more Ga solution is added to the water, and the increasing amount of Ga does not have an obvious suppression effect on the matrix effect of Cu isotope. However, adding water aerosol alone has significantly reduce the matrix effect during Cu isotope analysis (Figure S2), and the results are completely consistent with the results of adding water and Ga at the same time.

3.5 The effect of water introduction rate

The water aerosol was introduced into MC-ICP-MS through a nebulizer with argon (add gas), the amount of water can be

changed by adjusting the flow rate of the add gas. After changing the add gas, the sample gas flow rate needs to be retuned to obtain the maximum Cu and Ga intensities. When the argon flow rate (add gas) is 0.3 L min^{-1} (the water introduction rate is about 8.6 μL min^{-1}), the mean δ^{65}Cu value of TC1725 calibrated against NWU-Cu-B is –0.04±0.05‰ (n=5, 2SD), which is indistinguishable within measurement uncertainty from the solution result of –0.06±0.03‰ (2SD). Compared with the results under dry plasma, the data clearly show that the addition of water has significantly reduced the matrix effect of non-matrix-matched standardization. However, with the increase of water addition, the δ^{65}Cu values of chalcopyrite TC1725 calibrated by NWU-Cu-B are biased towards lighter delta values than that of the solution. When increasing the amount of water to 14.5 μL min^{-1} (add gas flow rate is 0.4 L min^{-1}), the acquired mean δ^{65}Cu value of TC1725 deviated to –0.16±0.04‰ (n=6, 2SD). Beyond this amount of water aerosol, the mean δ^{65}Cu value remains stable with a further increase of water amount. Thus, for the non-matrix-matched standardization, an accurate δ^{65}Cu value can be obtained at 8.6 μL min^{-1} water addition rate (Figure 6).

Matrix effect of LA-MC-ICP-MS is known as originated during laser ablation process, aerosol transport, ICP ionization, ion extraction, and depends on the composition and concentration of the sample matrix (Jackson and Günther, 2003; Agatemor and Beauchemin, 2011). For fs-LA-MC-ICP-MS, there is very little isotopic fractionation that occurs during laser ablation and transmission (Lin et al., 2019). Figure S3 shows the morphologies of ablation craters and deposited particles from CPY-SG (chalcopyrite) and NWU-Cu-B (pure copper) generated by a 206 nm femtosecond laser. The craters were ablated for 100 pulses at a repetition rate of 8 Hz and an energy density of 0.5 J cm^{-2}. As shown in Figure S3, there is a small amount of melted ejecta around the crater of CPY-SG, and almost no melted ejecta around the crater of NWU-Cu-B. Most aerosol particles are taken away with the carrier gas, rather than condensed around the crater. Significant melting phenomenon was not observed during femtosecond laser ablation, illustrating the thermal effects and isotopic fractionation of femtosecond laser are dramatically lower than that of nanosecond laser. The matrix effect mainly originated from the composition-related space charge effects in mass spectrometry, because femtosecond laser tends to produce finer and mono-modal particles, which can be quantitative ionized in the ICP (Agatemor and Beauchemin, 2011; Poitrasson and d'Abzac, 2017; Zheng et al., 2018).

Furthermore, under wet plasma condition the signal sensitivity decreases compared to that in dry plasma condition, which is also contradictory to the speculation that water may be improving the temperature of the plasma and the ionization efficiency of particles (Alder et al., 1980). Therefore, the effect of water is probably related to its effect on the space charge effect to a certain extent. To further investigate the effect of the water, pure copper solution (NWU-Cu-A) was used as an unknown sample and calibrated by pure copper solution NWU-Cu-B by solution nebulization MC-ICP-MS. Single standard solutions of Fe and S was added to NWU-Cu-A (Cu:Fe:S =1:1:1, molar ratio) to simulate the matrix of chalcopyrite. During the solution nebulizer MC-ICP-MS analysis, the δ^{65}Cu value of NWU-Cu-A with additional Fe and S (without Ga doping) is in good agreement with that of pure copper solution within uncertainty (Table 4), which is consistent with our previous research that the matrix effect can be ignored during solution nebulizer MC-ICP-MS analysis of Cu isotope in copper-bearing minerals (Lv et al., 2020; Zhang et al., 2020). An Aridus 3 desolvating nebulizer system (Teledyne CETAC Technologies, USA) was used here to remove solvent and introduce the NWU-Cu-A in dry plasma condition. Under dry plasma condition, the δ^{65}Cu value of NWU-Cu-A calibrated by NWU-Cu-B agreed with the preferred value (0.91±0.03‰ (Yuan et al., 2017)); however, after adding matrix elements Fe and S, the difference of δ^{65}Cu value of NWU-Cu-A from the preferred value is up to 0.76‰ (Table 4). Thus, compared with the "dry" plasma, the "wet" plasma is more robust and more tolerant to the matrix. The matrix effect becomes more severe in dry plasma condition even if the sample aerosol is formed by nebulizer rather than the laser ablation system, so it is considered that the water mainly affects the ICP ionization process and ion extraction process, and the matrix effect of Cu isotopes is reduced under the condition of wet plasma. Although many studies have applied the wet plasma to suppress the matrix effect, it is still difficult to fully investigate the detailed mechanism at present. further investigation on the detailed mechanism is still needed.

3.6 Long-term analytical reproducibility

The long-term reproducibility of our copper isotope analysis was tested on a repeated determination of δ^{65}Cu values for CPY-1 and TC1725 over a 6-month period, including matrix-matched calibration under dry plasma condition and non-matrix-matched calibration under wet plasma condition. The δ^{65}Cu values of CPY-1 and TC1725 are illustrated in Figure 7. For dry plasma condition, the CPY-1 was calibrated using the SSB method and the chalcopyrite TC1725 was adopted as the bracketing standard. The Cu isotopic results obtained by the fs-LA-MC-ICP-MS yield an average δ^{65}Cu value of 0.05±0.07‰ (n=75, 2SD), which agrees well with the previous data of solution analysis (0.05±0.02‰, n=4, 2SD). For wet plasma condition, the TC1725 was calibrated using the SSB combined with the internal standard Ga, while the pure copper NWU-Cu-B was used here as a non-matrix matched standard. The mean δ^{65}Cu value of non-matrix-matched calibration using fs-LA-MC-ICP-MS was −0.07±0.10‰

Table 4 δ^{65}Cu value of NWU-Cu-A under wet and dry plasma condition[a)]

	NWU-Cu-A			NWU-Cu-A +Fe+S (1:1:1)		
	δ^{65}Cu	2SD	*n*	δ^{65}Cu	2SD	*n*
Wet plasma	0.91	0.03	3	0.95	0.03	3
Dry plasma	0.87	0.01	3	0.15	0.04	3

a) These results were all measured without Ga doping.

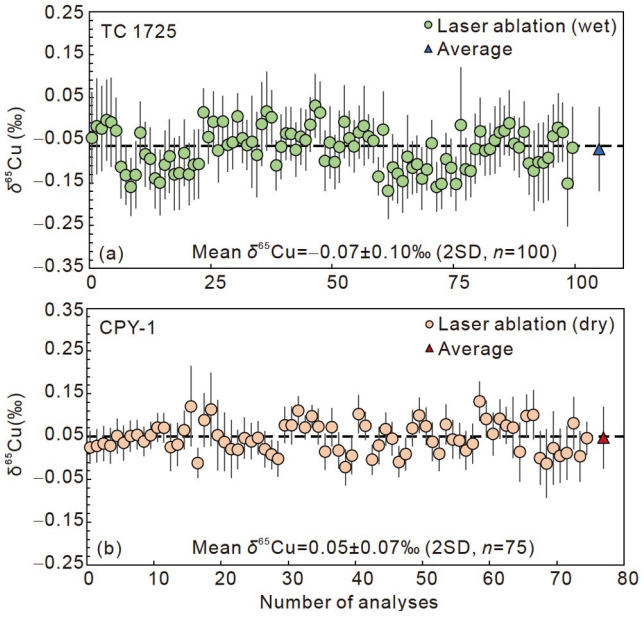

Figure 7 The long-term reproducibility of laser ablation Cu isotope analysis of chalcopyrite TC1725 and CPY-1. (a) δ^{65}Cu of TC1725 non-matrix-matched calibration under wet plasma condition; (b) δ^{65}Cu of CPY-1 matrix-matched calibration under dry plasma condition. Error bars for single analyses are 2SE and for average values are 2SD. The dotted line represents the solution value.

(*n*=100, 2SD) for TC1725 over a 6-month period, which is consistent with the preferred value obtained by solution nebulization MC-ICP-MS (–0.06±0.03‰ (Bao et al., 2021)). The data summarized here have demonstrated that the non-matrix-matched calibration of Cu isotope using fs-LA-MC-ICP-MS is applicable for copper-bearing minerals with long-term reproducibility <0.1‰, and the precision of both matrix-matched and non-matrix-matched calibrations of fs-LA-MC-ICP-MS using the SSB technique and the SSB combining internal standard Ga technique are comparable to solution nebulization MC-ICP-MS.

4. Conclusion

Cu, isotopic compositions of copper-rich minerals, were analyzed using the 206 nm femtosecond laser MC-ICP-MS. Matrix-matched reference materials are needed because the matrix effect results in a deviation of δ^{65}Cu up to 1.42‰ when using chalcopyrite to calibrate the pure copper, while precise (2SD<0.07‰) and accurate Cu isotope ratios can be acquired using matrix-matched standardization. In addition, lower fluence (<1 J cm^{-2}) and proper frequency (6–10 Hz) can reduce the effect of laser-induced Cu isotope fractionation. However, the matrix effect can be significantly suppressed by adding 8.6 μL min^{-1} water into the carrier gas. Consequently, reliable non-matrix-matched Cu isotope determination can be routinely achieved using the 206 nm fs-LA-MC-ICP-MS with a *long*-term precision of <0.1‰ (2SD), no matter the pure copper or the chalcopyrite were used as the bracketing standard. Non-matrix-matched calibration has expanded the application of *in situ* copper isotope measurement on typical Cu ore minerals with high resolution and comparable precision to solution nebulization MC-ICP-MS.

Acknowledgements *We thank two anonymous reviewers for their insightful and detailed comments, which significantly enhanced the manuscript. This work was supported by the National Natural Science Foundation of China (Grant Nos. 41825007, 42130102, 42073051, 42173033) and the MOST Research Foundation from the State Key Laboratory of Continental Dynamics.*

References

Agatemor C, Beauchemin D. 2011. Matrix effects in inductively coupled plasma mass spectrometry: A review. Anal Chim Acta, 706: 66–83
Alder J F, Bombelka R M, Kirkbright G F. 1980. Electronic excitation and ionization temperature measurements in a high frequency inductively coupled argon plasma source and the influence of water vapour on plasma parameters. Spectrochim Acta Part B-Atomic Spectr, 35: 163–175
Allner S, Koch J, Jackson S E, Günther D. 2017. Effects of H_2O- and O_2-containing He carrier gases on the $^{206}Pb/^{238}U$ system bias and downhole fractionation in LA-ICPMS of zircon. J Anal At Spectrom, 32: 2238–2245
Aramendía M, Rello L, Resano M, Vanhaecke F. 2013. Isotopic analysis of Cu in serum samples for diagnosis of Wilson's disease: A pilot study. J Anal At Spectrom, 28: 675
Bao Z A, Lv N, Chen K Y, Luan Y, Sun X H, Zong C L, Yuan H L. 2021. A potential new chalcopyrite reference material for LA-MC-ICP-MS copper isotope ratio measurement. Geostand Geoanal Res, 45: 401–418
Borrok D M, Wanty R B, Ridley W I, Wolf R, Lamothe P J, Adams M. 2007. Separation of copper, iron, and zinc from complex aqueous solutions for isotopic measurement. Chem Geol, 242: 400–414
Brzozowski M J, Good D J, Wu C, Li W. 2020. Cu isotope systematics of conduit-type Cu-PGE mineralization in the Eastern Gabbro, Coldwell Complex, Canada. Miner Depos, 56: 707–724
Chiaradia M. 2014. Copper enrichment in arc magmas controlled by overriding plate thickness. Nat Geosci, 7: 43–46
d'Abzac F X, Beard B L, Czaja A D, Konishi H, Schauer J J, Johnson C M. 2013. Iron isotope composition of particles produced by UV-femtosecond laser ablation of natural oxides, sulfides, and carbonates. Anal Chem, 85: 11885–11892
Fu J, Hu Z, Zhang W, Yang L, Liu Y, Li M, Zong K, Gao S, Hu S. 2016. *In situ* sulfur isotopes (δ^{34}S and δ^{33}S) analyses in sulfides and elemental sulfur using high sensitivity cones combined with the addition of nitrogen by laser ablation MC-ICP-MS. Anal Chim Acta, 911: 14–26
Graham S, Pearson N, Jackson S, Griffin W, O'Reilly S Y. 2004. Tracing Cu and Fe from source to porphyry: *In situ* determination of Cu and Fe isotope ratios in sulfides from the Grasberg Cu-Au deposit. Chem Geol, 207: 147–169
Hill S J, Ford M J, Ebdon L. 1992. Simplex optimization of nitrogen-argon

plasmas in inductively coupled plasma mass spectrometry for the removal of chloride-based interferences. J Anal At Spectrom, 7: 719–725
Hirayama Y, Obara M. 2005. Heat-affected zone and ablation rate of copper ablated with femtosecond laser. J Appl Phys, 97: 064903
Hou Q H, Zhou L, Gao S, Zhang T, Feng L, Yang L. 2016. Use of Ga for mass bias correction for the accurate determination of copper isotope ratio in the NIST SRM 3114 Cu standard and geological samples by MC-ICPMS. J Anal At Spectrom, 31: 280–287
Hu Z, Gao S, Liu Y, Hu S, Chen H, Yuan H. 2008. Signal enhancement in laser ablation ICP-MS by addition of nitrogen in the central channel gas. J Anal At Spectrom, 23: 1093
Ikehata K, Hirata T. 2013. Evaluation of UV-fs-LA-MC-ICP-MS for precise *in situ* copper isotopic microanalysis of cubanite. Anal Sci, 29: 1213–1217
Ikehata K, Notsu K, Hirata T. 2008. *In situ* determination of Cu isotope ratios in copper-rich materials by NIR femtosecond LA-MC-ICP-MS. J Anal At Spectrom, 23: 1003
Jackson S E, Günther D. 2003. The nature and sources of laser induced isotopic fractionation in laser ablation-multicollector-inductively coupled plasma-mass spectrometry. J Anal At Spectrom, 18: 205–212
Jouvin D, Weiss D J, Mason T F M, Bravin M N, Louvat P, Zhao F, Ferec F, Hinsinger P, Benedetti M F. 2012. Stable isotopes of Cu and Zn in higher plants: Evidence for Cu reduction at the root surface and two conceptual models for isotopic fractionation processes. Environ Sci Technol, 46: 2652–2660
Kuhn H R, Pearson N J, Jackson S E. 2007. The influence of the laser ablation process on isotopic fractionation of copper in LA-MC-ICP-MS. J Anal At Spectrom, 22: 547
Lazarov M, Horn I. 2015. Matrix and energy effects during *in-situ* determination of Cu isotope ratios by ultraviolet-femtosecond laser ablation multicollector inductively coupled plasma mass spectrometry. Spectrochim Acta Part B-Atomic Spectr, 111: 64–73
Lee C T A, Luffi P, Chin E J, Bouchet R, Dasgupta R, Morton D M, Le Roux V, Yin Q, Jin D. 2012. Copper systematics in arc magmas and implications for crust-mantle differentiation. Science, 336: 64–68
Li W, Jackson S E, Pearson N J, Graham S. 2010. Copper isotopic zonation in the Northparkes porphyry Cu-Au deposit, SE Australia. Geochim Cosmochim Acta, 74: 4078–4096
Lin J, Liu Y, Hu Z, Chen W, Zhang C, Zhao K, Jin X. 2019. Accurate analysis of Li isotopes in tourmalines by LA-MC-ICP-MS under "wet" conditions with non-matrix-matched calibration. J Anal At Spectrom, 34: 1145–1153
Liu S A, Li D, Li S, Teng F Z, Ke S, He Y, Lu Y. 2014. High-precision copper and iron isotope analysis of igneous rock standards by MC-ICP-MS. J Anal At Spectrom, 29: 122–133
Luo T, Hu Z, Zhang W, Liu Y, Zong K, Zhou L, Zhang J, Hu S. 2018. Water vapor-assisted "universal" nonmatrix-matched analytical method for the *in situ* U-Pb dating of zircon, monazite, titanite, and xenotime by laser ablation-inductively coupled plasma mass spectrometry. Anal Chem, 90: 9016–9024
Lv N, Bao Z, Chen L, Chen K, Zhang Y, Yuan H. 2020. Accurate determination of Cu isotope compositions in Cu-bearing minerals using microdrilling and MC-ICP-MS. Int J Mass Spectrometry, 457: 116414
Lv N. 2021. *In situ* analysis of copper isotopes in copper-bearing minerals by femtosecond laser ablation MC-ICP-MS (in Chinese). Doctoral Dissertation. Northwest University
Machlan L A, Gramlich J W, Powell L J, Lambert G M. 1986. Absolute isotopic abundance ratio and atomic weight of a reference sample of gallium. J ResNatlBurStand, 91: 323
Maher K C, Larson P B. 2007. Variation in copper isotope ratios and controls on fractionation in hypogene skarn mineralization at Coroccohuayco and Tintaya, Peru. Econ Geol, 102: 225–237
Markl G, Lahaye Y, Schwinn G. 2006. Copper isotopes as monitors of redox processes in hydrothermal mineralization. Geochim Cosmochim Acta, 70: 4215–4228
Mathur R, Ruiz J, Casselman M J, Megaw P, van Egmond R. 2012. Use of Cu isotopes to distinguish primary and secondary Cu mineralization in the Cañariaco Norte porphyry copper deposit, Northern Peru. Miner Depos, 47: 755–762
Moynier F, Vance D, Fujii T, Savage P. 2017. The isotope geochemistry of zinc and copper. Rev Mineral Geochem, 82: 543–600
Oeser M, Weyer S, Horn I, Schuth S. 2014. High-precision Fe and Mg isotope ratios of silicate reference glasses determined *in situ* by femtosecond LA-MC-ICP-MS and by solution nebulisation MC-ICP-MS. Geostand Geoanal Res, 38: 311–328
Poitrasson F, d'Abzac F X. 2017. Femtosecond laser ablation inductively coupled plasma source mass spectrometry for elemental and isotopic analysis: Are ultrafast lasers worthwhile? J Anal At Spectrom, 32: 1075–1091
Roebbert Y, Rabe K, Lazarov M, Schuth S, Schippers A, Dold B, Weyer S. 2018. Fractionation of Fe and Cu isotopes in acid mine tailings: Modification and application of a sequential extraction method. Chem Geol, 493: 67–79
Rouxel O, Fouquet Y, Ludden J N. 2004. Copper isotope systematics of the lucky strike, Rainbow, and logatchev sea-floor hydrothermal fields on the Mid-Atlantic ridge. Econ Geol, 99: 585–600
Ryan B M, Kirby J K, Degryse F, Harris H, McLaughlin M J, Scheiderich K. 2013. Copper speciation and isotopic fractionation in plants: Uptake and translocation mechanisms. New Phytol, 199: 367–378
Schuessler J A, von Blanckenburg F. 2014. Testing the limits of micro-scale analyses of Si stable isotopes by femtosecond laser ablation multicollector inductively coupled plasma mass spectrometry with application to rock weathering. Spectrochim Acta Part B-Atomic Spectr, 98: 1–18
Seo J H, Lee S K, Lee I. 2007. Quantum chemical calculations of equilibrium copper (I) isotope fractionations in ore-forming fluids. Chem Geol, 243: 225–237
Shields W R, Goldich S S, Garner E L, Murphy T J. 1965. Natural variations in the abundance ratio and the atomic weight of copper. J Geophys Res, 70: 479–491
Sullivan K, Layton-Matthews D, Leybourne M, Kidder J, Mester Z, Yang L. 2020. Copper isotopic analysis in geological and biological reference materials by MC-ICP-MS. Geostand Geoanal Res, 44: 349–362
Yang S C, Welter L, Kolatkar A, Nieva J, Waitman K R, Huang K F, Liao W H, Takano S, Berelson W M, West A J, Kuhn P, John S G. 2019. A new anion exchange purification method for Cu stable isotopes in blood samples. Anal Bioanal Chem, 411: 765–776
Yuan H, Yuan W, Bao Z, Chen K, Huang F, Liu S. 2017. Development of two new copper isotope standard solutions and their copper isotopic compositions. Geostand Geoanal Res, 41: 77–84
Zhang Y, Bao Z, Lv N, Chen K, Zong C, Yuan H. 2020. Copper isotope ratio measurements of Cu-dominated minerals without column chromatography using MC-ICP-MS. Front Chem, 8: 609
Zhao Y, Xue C, Liu S A, Symons D T A, Zhao X, Yang Y, Ke J. 2017. Copper isotope fractionation during sulfide-magma differentiation in the Tulaergen magmatic Ni-Cu deposit, NW China. Lithos, 286-287: 206–215
Zheng X Y, Beard B L, Johnson C M. 2018. Assessment of matrix effects associated with Fe isotope analysis using 266 nm femtosecond and 193 nm nanosecond laser ablation multi-collector inductively coupled plasma mass spectrometry. J Anal At Spectrom, 33: 68–83
Zhu X K, Makishima A, Guo Y, Belshaw N S, O'Nions R K. 2002. High precision measurement of titanium isotope ratios by plasma source mass spectrometry. Int J Mass Spectrometry, 220: 21–29
Zhu Z Y, Jiang S Y, Ciobanu C L, Yang T, Cook N J. 2017. Sulfur isotope fractionation in pyrite during laser ablation: Implications for laser ablation multiple collector inductively coupled plasma mass spectrometry mapping. Chem Geol, 450: 223–234

(Responsible editor: Yueheng YANG)